
PaccMann: Prediction of anticancer compound sensitivity with multi-modal attention-based neural networks

Ali Oskooei^{*1}, Jannis Born^{*1,2,3}, Matteo Manica^{*1,3},
Vigneshwari Subramanian⁴, Julio Sáez-Rodríguez^{4,5}, María Rodríguez Martínez¹

¹IBM Research, Zürich, Switzerland, ²University of Zürich, ³ETH Zürich,
⁴RWTH Aachen University, Aachen, Germany, ⁵Heidelberg University, Heidelberg, Germany

Abstract

We present a novel approach for the prediction of anticancer compound sensitivity by means of multi-modal attention-based neural networks (PaccMann). In our approach, we integrate three key pillars of drug sensitivity, namely, the molecular structure of compounds, transcriptomic profiles of cancer cells as well as prior knowledge about interactions among proteins within cells. Our models ingest a drug-cell pair consisting of SMILES encoding of a compound and the gene expression profile of a cancer cell and predicts an IC50 sensitivity value. Gene expression profiles are encoded using an attention-based encoding mechanism that assigns high weights to the most informative genes. We present and study three encoders for SMILES string of compounds: 1) bidirectional recurrent 2) convolutional 3) attention-based encoders. We compare our devised models against a baseline model that ingests engineered fingerprints to represent the molecular structure. We demonstrate that using our attention-based encoders, we can surpass the baseline model. The use of attention-based encoders enhance interpretability and enable us to identify genes, bonds and atoms that were used by the network to make a prediction.

1 Introduction

Invention of novel compounds with a desired efficacy and improving existing therapies are key bottlenecks in the pharmaceutical industry, which fuel the largest R&D business spending of any industry and account for 19% of the total R&D spending worldwide [1, 2]. Anticancer compounds, in particular, take the lion’s share of drug discovery R&D efforts, with over 34% of all drugs in the global R&D pipeline in 2018 (5,212 of 15,267 drugs) [3]. Despite enormous scientific and technological advances in recent years, serendipity still plays a major role in anticancer drug discovery [4] without a systematic way to accumulate and leverage years of R&D to achieve higher success rates in drug discovery.

On the other hand, there is strong evidence that the response to anticancer therapy is highly dependent on the tumor genomic and transcriptomic makeup, resulting in heterogeneity in patient clinical response to anticancer drugs [5, 6]. This varied clinical response has led to the promise of personalized (or precision) medicine in cancer, where molecular biomarkers, e.g., the expression of specific genes, obtained from a patient’s tumor profiling may be used to choose a personalized therapy. These challenges highlight a need across both pharmaceutical and health care industries for multi-modal quantitative methods that can jointly exploit disparate sources of knowledge with the goal of

*Shared first-authorship. {osk,jab,tte}@zurich.ibm.com

characterizing the link between the molecular structure of compounds, the genetic and epigenetic alterations of the biological samples and drug response. There have been a plethora of works focused on prediction of drug sensitivity in cancer cells [5, 7, 8], however, the majority of them have focused on the analysis of unimodal datasets such as genomic or transcriptomic profiles of cancer cells. A few models have proposed the integration of two different data modalities, e.g., genomic features and chemical descriptors [9].

Chemical descriptors and fingerprints are engineered features that describe the chemical properties and structure of a compound. Chemical descriptors have been extensively used in the chemical and biological engineering domain to develop quantitative structure-activity relationship (QSAR) and quantitative structure-property relationship (QSPR) models of compounds [10]. Similarly, molecular fingerprints (FP) have been extensively applied to drug discovery, virtual screening and compound similarity search [11]. Even though chemical descriptors and fingerprints have found many applications in combination with machine learning algorithms, the usage of engineered features limit the learning ability of such algorithms and may prove problematic in applications where these features are not relevant or informative [2].

With the rise of deep learning methods and their proven ability to learn the most informative features from raw data, it seems imperative to approach chemical problems from a similar standpoint. Recently, methods borrowed from neural language models [12] have been used in combination with SMILES string encoding of molecules to successfully predict chemical properties of molecules [2, 13] or products of a chemical reaction [14]. To the best of our knowledge there have not been any multi-modal deep learning solutions for anticancer drug sensitivity prediction that combine molecular structure of compounds, genetic profile of cells and prior knowledge of protein interactions. It is timely that utility of such a model be systematically explored and demonstrated. We address this gap in the current work. Specifically, we explore neural feature learning from raw SMILES encoding of chemicals (as opposed to engineered features) in the context of drug sensitivity in cancer cells (see Figure 1). We validate our models against a baseline feedforward model based on the Morgan (Circular) chemical fingerprints [15]. In doing so, we demonstrate that the direct analysis of raw SMILES encodings through an attention-based architecture can surpass the performance of models based on fingerprints. This is highly desirable, as SMILES are accessible and intuitively more interpretable.

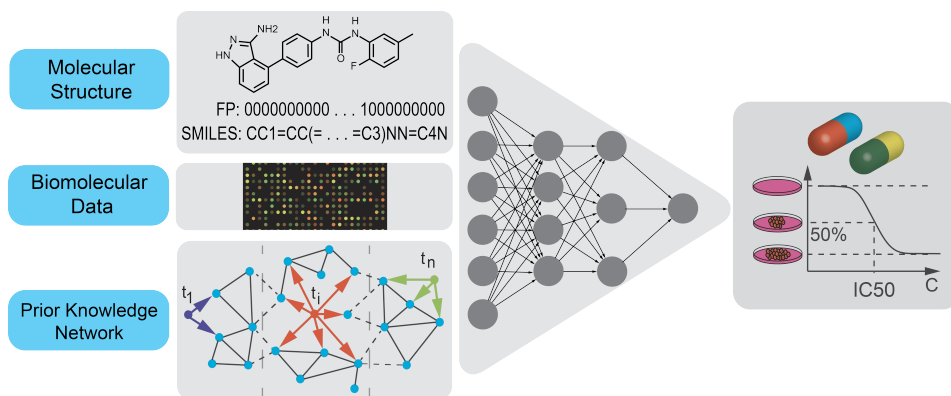


Figure 1: **Multi-modal prediction of IC50 drug sensitivity.** Three key data modalities that influence anticancer drug sensitivity: biomolecular measurements of cancer cells (gene expression, copy number alteration etc.), a network of known interactions between the biomolecular entities and the chemical structure of the anticancer compounds.

2 Methods

2.1 Data

Throughout this work, we employed the gene expression and drug IC50 data publicly available as part of the Genomics of Drug Sensitivity in Cancer (GDSC) database [5, 6]. The dataset includes the results of screening on more than a thousand genetically profiled human pan-cancer cell lines with a wide range of anticancer compounds. The screened compounds include chemotherapeutic drugs

as well as targeted therapeutics from various sources [6]. We based our models on gene expression data, as it has been shown to be more predictive of drug sensitivity than genomics (i.e., copy number variation and mutations) or epigenomics (i.e., methylation) data [16, 17, 7]. STRING protein-protein interaction (PPI) network [18] was used to incorporate intracellular interactions in our model. Within the GDSC database, 221 compounds were targeted therapies, which are the focus of our work. Of 221 compounds, the molecular structures of 208 compounds were publicly available. For the 208 compounds with publicly available molecular structure, we collected canonical SMILES and acquired Morgan fingerprints using RDKit². Exploiting the property that most molecules have multiple valid SMILES strings, we adopted a data augmentation strategy [19] and represented each anticancer compound with 32 SMILES strings. This results in a dataset consisting of 6,556,160 drug-cell pairs.

2.2 Network propagation

Network propagation was employed to reduce the dimensionality of the cell lines’ transcriptomic profile, consisting of 16,000 genes, to a smaller subset containing the most informative genes [17]. We identify the most relevant genes by employing a weighting and network propagation scheme: we first assign a high weight ($W = 1$) to the reported drug target genes while assigning a very small positive weight ($\varepsilon = 1e-5$) to all other genes. Thereafter, the initialized weights are propagated over the STRING protein-protein-interaction (PPI) network [18], a comprehensive PPI database including interactions from multiple data sources. This process is meant to integrate prior knowledge about molecular interactions into our weighting scheme, and simulates the propagation of perturbations within the cell following the drug administration. The network smoothing of the weights can be described as a random walk, starting from the initial drug target weights, throughout the network. More specifically, let us denote the initial weights as W_0 and the string network as $S = (P, E, A)$, where P are the protein vertices of the network, E are the edges between the proteins and A is the weighted adjacency matrix, a matrix that indicates the level of confidence about the existence of a certain interaction. The smoothed weights are determined from an iterative solution of the propagation function [17]:

$$W_{t+1} = \alpha W_t A' + (1 - \alpha) W_0 \quad \text{where} \quad A' = D^{-\frac{1}{2}} A D^{-\frac{1}{2}} \quad (1)$$

where D is the degree matrix and A' is the normalized adjacency matrix. The diffusion tuning parameter, α ($0 \leq \alpha \leq 1$), defines how far the prior knowledge weights can diffuse through the network. In this work, we used $\alpha = 0.7$, as recommended in the literature for the STRING network [20]. Adopting a convergence rule of $e = (W_{t+1} - W_t) < 1e-6$, we solved Equation 1 iteratively for each drug and used the resultant weights distribution to determine the top 20 highly ranked genes for each drug. We then pooled the top 20 genes for all 208 compounds, resulting in a subset of 2,128 genes. This subset containing the most informative genes was then used to profile each cell line in the dataset before it was fed into our models.

2.3 Model architectures

The general architecture of our model is shown in Figure 2. To predict drug sensitivity we adopted two architecture configurations to ingest the different molecular structure encodings:

Fingerprint models. We selected fingerprint-based models as the baseline comparison for all the considered model configurations. Fingerprint representations of molecular structure have been proven to be a highly informative, and can therefore serve as a reliable reference [21, 22]. Our baseline model is a 6-layered DNN with [512, 256, 128, 64, 32, 16] units and a sigmoidal activation designed by optimizing hyperparameters following a cross-validation scheme (see subsection 2.4). The genetic profiles are filtered using the network propagation process described in subsection 2.2, and ingested in conjunction with 512-bit Morgan fingerprints as the encoding of the compound structure.

SMILES models. These models ingest the filtered gene expression profiles and the SMILES text encodings for the structure of the compounds. To encode the SMILES, we employed 5 models falling into 3 general categories: recurrent, convolutional and pure attention-based encoders (see Figure 2).

The genetic subset selected through network propagation is further processed using a gene attention encoder (GAE), see Figure 3A. This architecture produces weights for each of the genes and applies these weights to the genes in a dot product, ensuring most informative genes receive a higher weight. In addition, the resulting gene weights render the model more interpretable, as it identifies the genes

²<https://github.com/rdkit/rdkit>

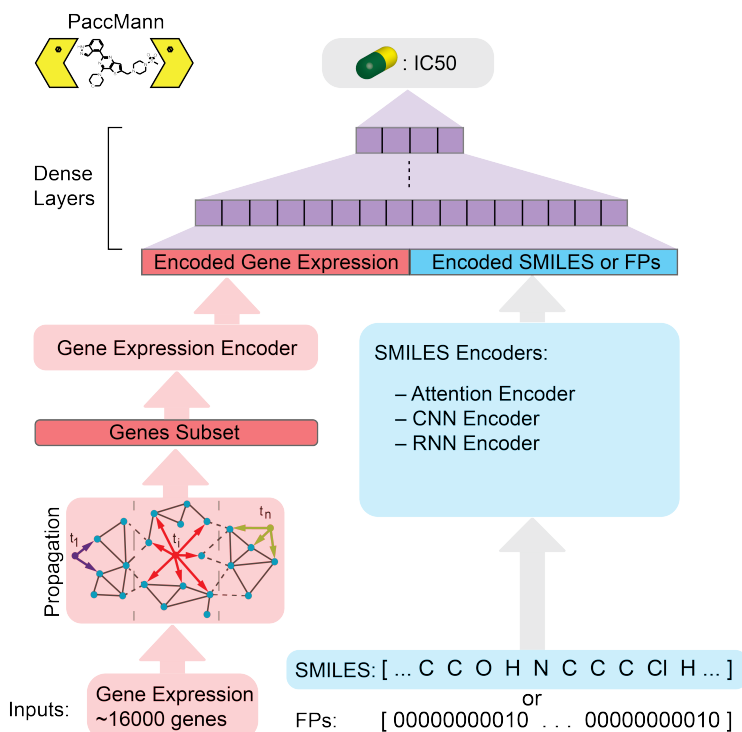


Figure 2: **The end-to-end architecture of PaccMann.** PaccMann ingests a cell-compound pair and makes a IC50 drug sensitivity prediction for the pair. Cells are represented by the gene expression values of a subset of 2,128 genes, selected for having the highest weights following the network propagation. Compound structures are represented either as 512 bit fingerprint or in the SMILES formats. The gene-vector is fed into an attention-based encoder that assigns higher weights to the most informative genes. Fingerprints are used in combination with the gene expression subset in a dense baseline model. SMILES encoding of compounds is employed by an array of encoders that are combined with a representation of gene expression to obtain a drug sensitivity prediction.

that drive the sensitivity prediction in each cell line. To ensure charged or multi-character atoms (e.g., Cl or Br) were added as distinct tokens to the dictionary, the SMILES sequences were tokenized using a regular expression [14]. The resulting atomic sequences of length T are represented as $E = \{e_1, \dots, e_T\}$, with learned embedding vectors e_i of length H for each dictionary token (see Figure 3B).

To investigate which model architecture best exploits the drug compound information, we explored various SMILES encoders, starting with a 2-layered bidirectional recurrent neural network (bRNN) that utilized gated recurrent units (GRU) [23]. Next, we employed a stacked convolutional encoder (SCNN) with 4 layers and a sigmoidal activation function. Whilst 2D convolutions in the first layer collapsed the embedding hidden dimensionality, subsequent 1D convolutions extracted incrementally increasing long-range interactions between different parts of the molecule.

As previously mentioned, we employed encoders that leveraged attention mechanisms. Interpretability is paramount in medicinal and machine learning applications to the health domain [24]. As such, attention in particular, is central in our models as it enables us to explain and interpret the observed results in the context of underlying biological and chemical processes. As such, we explored different attention-based encoders in our models. The first attention configuration we adopted is a self-attention (SA) mechanism originally developed for document classification [25] and here adapted to SMILES representations (see Figure 3C). The attention weights α_i were computed as:

$$\alpha_i = \frac{\exp(u_i)}{\sum_j^T u_j} \quad \text{where} \quad u_i = V^T \tanh(W_e e_i + b) \quad (2)$$

The matrix $W_e \in \mathbb{R}^{A \times H}$ and the bias vector $b \in \mathbb{R}^{A \times 1}$ are learned in a dense layer. The learned vector V combines the atom annotations from the attention space, through a dot product the output of which is fed to a softmax layer, to obtain the SMILES attention weights.

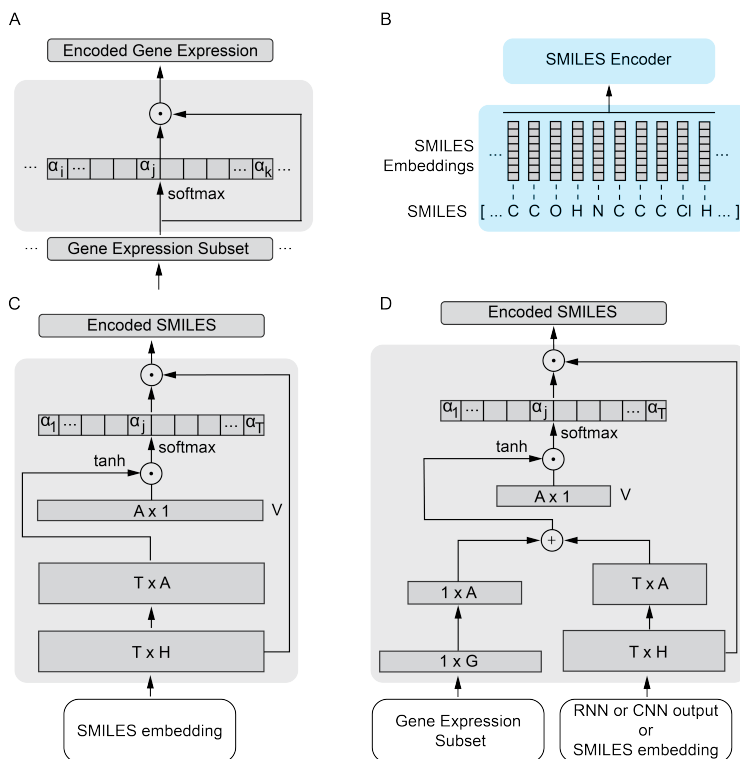


Figure 3: **The architecture of various encoders used in PaccMann.** A) An attention-based gene expression encoder generates attention weights that are in turn applied to the input gene subset via a dot product. B) An embedding layer transforms raw SMILES strings into a sequence of vectors in an embedding space. C) A self-attention SMILES encoder ingests the SMILES embeddings and computes attention weights, α_i , that is used to combine the inputs into a single vector of hidden dimensionality H . D) SMILES encoder with an attention process similar to Bahdanau’s, where the target hidden states are replaced by a context vector representing the gene expression subset [12]. The model learns to give higher weights to SMILES tokens that have the most influence given the gene expression of the cell, unlike the attention process described in C), where weights are determined based only on the SMILES.

Alternatively, we devised a contextual attention (CA) mechanism that utilizes the gene expression subset G as context in determining the attention weights α_i according to the following equation (see Figure 3D):

$$u_i = V^T \tanh(W_e e_i + W_g G) \quad \text{where} \quad W_g \in \mathbb{R}^{A \times |G|} \quad (3)$$

First, the matrices W_g and W_e project both genes G and the embedded sequence element e_i into the attention space, A . Adding the gene context vector to the projected token ultimately yields an α_i that takes into account the relevance of a compound substructure given a gene subset G .

In both attention mechanisms, the encoded smiles are obtained by filtering the inputs with the attention weights. However, operating directly on the embeddings, the attention-based encoder disregards positional information whilst exclusively exploring information of individual tokens (i.e., atoms and bonds). In an attempt to combine atomic and regional, submolecular interactions, we tested a (shallow) multichannel convolutional attentive encoder (MCA) with two parallel kernel sets of sizes $[H, 5]$ and $[H, 11]$. The resulting feature maps were fed to 2 separate contextual attention layers; a third one operated directly on the SMILES embedding so as to incorporate information from individual tokens. For all models, the output of the smiles encoder was concatenated with the output of the gene expression encoder before the regression was completed by a set of feedforward layers.

2.4 Model evaluation

We adopted a strict data split approach ensuring no cell line profile or compound structure within the validation or test set has been seen by our models prior to validation or testing. 10% subsets of the total number of 208 compounds and 985 cell lines from the GDSC database were set aside to be used

as an unseen test dataset to evaluate the trained models (as shown in Figure 4A). The remaining 90%

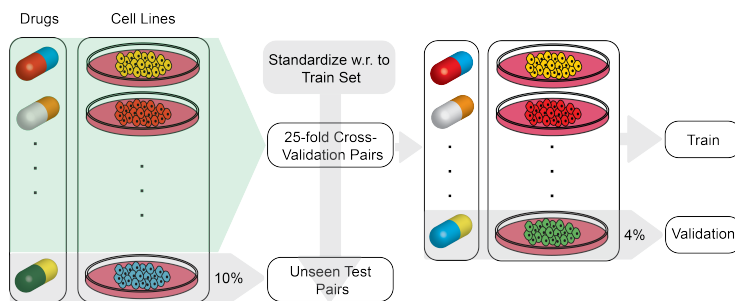


Figure 4: **Data preparation, split and model evaluation strategy.** We adopted a strict train-validation-test approach, ensuring that none of the cells and drugs in the test or validation set were seen by the trained model. All drugs and pan-cancer cell lines within the GDSC dataset were lined up and a 10% random subset of both drugs and cell lines were separated as test dataset. The remaining 90% of the drugs and cell lines were used for model training and evaluation in a 25-fold cross-validation scheme.

of compounds and cell lines were then used in a 25-fold cross-validation scheme for model training and validation. In each fold, 4% of the drugs and 4% of cell lines were separated as validation dataset and the remaining drugs and cell lines were paired and fed to the model for training, as shown in Figure 2A. Each drug in a subset (train, validation, test) was paired with gene expression profile (GEP) in the subset that the drug had been screened with. All models ingested the data as either FP-GEP or SMILES-GEP pairs and returned normalized IC50 drug sensitivity.

2.5 Training procedure

All described architectures were implemented in TensorFlow 1.10³ and optimized MSE with Adam ($\beta_1 = 0.9$, $\beta_2 = 0.999$, $\epsilon = 1e-8$) and a decreasing learning rate [26]. $H=16$ for all SMILES encoder and $A=256$ for all but the convolutional encoder (64). In the final dense layers of all models we employed dropout ($p_{drop} = 0.5$), batch normalization and a sigmoidal activation. All models were trained with a batch size of 2,048 for a maximum of 500k steps on a cluster equipped with POWER8 processors and a single NVIDIA Tesla P100.

3 Results

3.1 Performance comparison

Table 1 compares the test performance of all six models trained using a 25-fold cross validation scheme. The contextual attention models yielded on average the best performance in predicting drug sensitivity (IC50) of unseen drug-cell pairs. As IC50 was normalized to [0,1], the RMSE for the CA model implies an average deviation of 11% of the predicted IC50 values from the true values.

As the most prevalent technique to encode sequences, we found the bRNN to match but not surpass the performance of the baseline model. The SCNN, whose encoded feature maps consider information from even longer spatial segments of the SMILES than the bRNN (due to the stacking), performed significantly worse than the baseline, as assessed by a one-sided Mann-Whitney-U test ($U=126$, $p<2e-4$).

We therefore hypothesized the atomic features on the SMILES-token level (rather than submolecular interactions) to be most predictive of a drug’s efficacy (such as mere atom counts). Utilizing attention-based models that operated directly on the SMILES embedding, we extracted two models (SA, CA) that were superior to all others (e.g., CA vs. DNN: $U=42$, $p<9e-8$, SA vs. DNN: $U=82$, $p<5e-6$). Incorporating genomic information into the attention process (CA vs. SA) had not a *significant* effect on prediction performance. Surprisingly, neither complementing the SMILES embedding with positional encodings (like in Vaswani et al. [27]) nor adding the attention mechanism after the recurrent encoder was found to be beneficial for the presented models during the optimization

³<https://github.com/tensorflow/tensorflow>

Table 1: **Performance of the considered architectures on test data.** Results for all the architectures trained during the 25-fold cross validation process. The first column reports the best result in terms of RMSE between predicted and true IC50 values on test data, whereas the second column shows the average across all 25 models. Interestingly, attention-only models statistically significantly outperform all others, including models trained on fingerprints (star indicating a significance of $p < 0.01$ compared to the baseline encoder).

Encoder type	Drug structure	RMSE	
		Best	Average
Deep baseline (DNN)	Fingerprints	0.114	0.123 \pm 0.008
Bidirectional recurrent (bRNN)	SMILES	0.106	0.118 \pm 0.007
Stacked convolutional (SCNN)	SMILES	0.120	0.133 \pm 0.012
Self-attention (SA)	SMILES	0.089	0.112* \pm 0.007
Contextual attention (CA)	SMILES	0.095	0.110* \pm 0.008
Multichannel convolutional attentive (MCA)	SMILES	0.106	0.120 \pm 0.001

process on the cross-validation folds. Ultimately, the MCA model aimed towards complementing the token-level information (that was provably beneficial for the attention-only models), with spatially more holistic chemical features within the same model. However, the MCA is found to perform comparable to the bRNN, whilst not reaching the attention-only models. Overall, these results suggest that token-level (atoms, bonds) but not subregional information is most predictive for drug sensitivity.

3.2 Attention analysis

Considering the best SA model trained (RMSE=0.089 and Pearson correlation $\rho=0.66$ on the test data), we analyzed its predictions for a selection of drugs and cell lines included in the test set (see Table 2). The genes highlighted by the computed attention weights showed a significant enrichment [28, 29] of

Table 2: **IC50 prediction for a panel of ten cell-drug pairs**. Listed in the table are the predicted and true IC50 values for a selection of 10 unseen drug-cell pairs within the test dataset. In addition, the top-5 attended genes given by GAE are listed for each cell line.

Drug	Cell line	Cancer type	Top-5 attended genes	IC50	
				Predicted	Measured
Afatinib	UMC-11	lung (NSCLC)	F13A1, MYH4, ATOH8, SEMA4A, NES	0.505	0.493
BX-912	YH-13	glioma	RNASE2, HOXA13, CBR3, FABP1, HDC	0.532	0.5
GSK319347A	EW-12	bone	CD300A, RHBDL2, NES, TFF3, SOCS1	0.597	0.7
JW-7-24-1	OVTOKO	ovary	HDC, EIF2A, RNASE2, ANGPTL6, CBR3	0.502	0.49
PI-103	MV-4-11	leukemia	TFF3, ATOH8, RBP2, ITIH3, GRIP1	0.362	0.33
TGX221	SW962	urogenital system	CBR3, RNASE2, FABP1, HDC, SH3D21	0.621	0.66
S-Trityl-L-cysteine	NCI-H187	lung (SCLC)	RHBDL2, NR1H4, MYH4, NES, APCS	0.535	0.502
Fedratinib	BL-41	lymphoma	TFF3, ATOH8, RBP2, MAPK7, ARHGEF33	0.382	0.428
Tipifarnib	RCC10RGB	kidney	EIF2A, HDC, CBR3, PIK3R5, HOXA13	0.542	0.544
Midostaurin	GAK	skin	SVOP, FABP1, HDC, F13A1, FGFR3	0.507	0.477

the JAK-STAT signaling pathway, a known therapeutic target in cancer [30].

As a case study, we chose an anticancer compound from Table 2, Tipifarnib, and studied the SMILES attention weights given by the SA model. The attention weights for Tipifarnib are visualized in Figure 5. As shown in figure 5, rudimentary or frequent atoms such as C or H are given a negligible weight while chlorine is given the highest weight followed by the amid group, -NH2, O, N and the covalent bonds. As an additional case study, at the bottom of Figure 5, the STRING protein neighborhoods for top-weighted genes of two kidney cancer cell-lines are illustrated. Interestingly, even if the cell lines are not genomically identical, both computed attention weights underline the role of EIF2A, a key gene for tumor initiation [31].

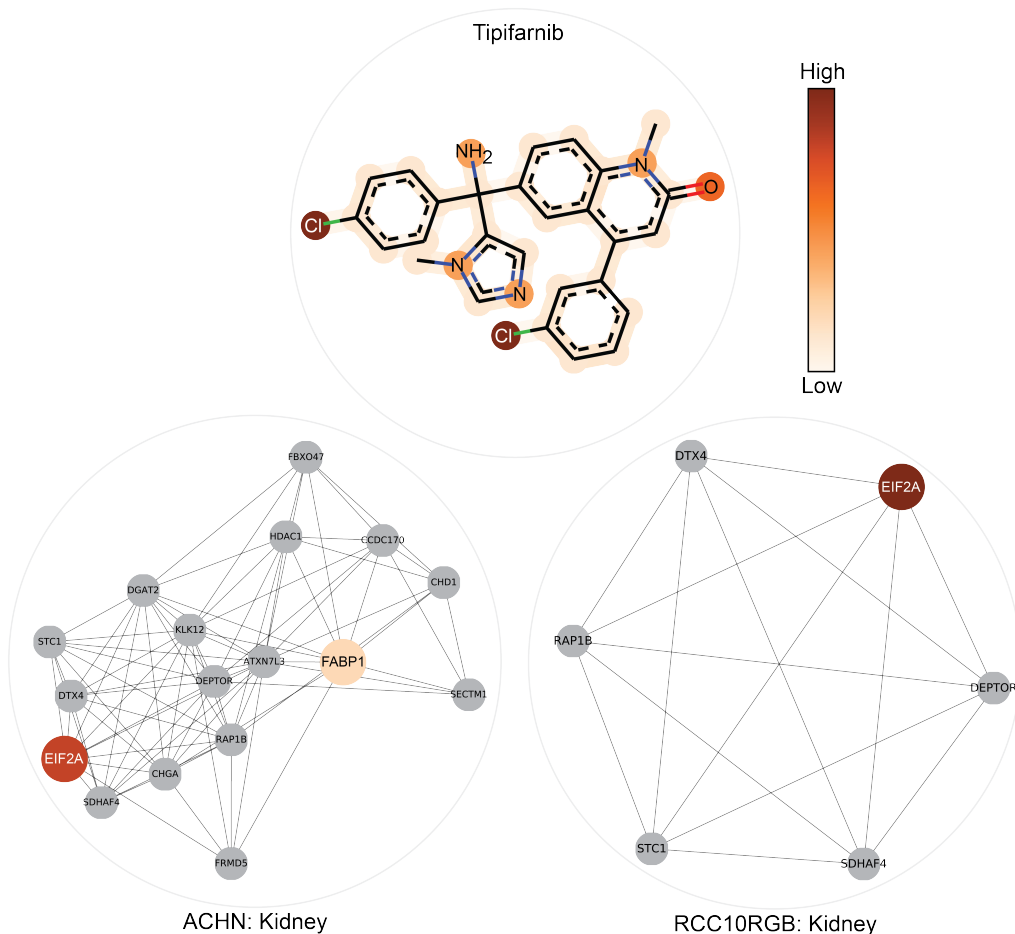


Figure 5: **Attention weights on genes and drugs.** We report here attention weights for Tipifarnib (top) and two kidney cell lines: ACHN (bottom left) and RCC10RGB (bottom right). The attention weights are computed using the best SA model with their intensity being encoded using an orange color map (light to dark). In Tipifarnib we highlight elements of the drug molecular structure using the learned weights. In the two cell lines we highlight genes with highest attention weights while displaying their neighborhood in the STRING networks.

4 Discussion

In this work, we presented a multi-modal approach to neural prediction of drug sensitivity based on a combination of 1) molecular structure of drug compounds 2) the gene expression profile of cancer cells and 3) intracellular interactions incorporated into a PPI network. We adopted a strict model evaluation approach in which we ensured that no cells or compounds in the validation or test datasets are ever seen by the trained model. Despite our strict evaluation strategy, our best model (CA) achieved an average standard deviation of 0.11 in predicting normalized IC50 values for unseen drug-cell pairs. We demonstrated that using the raw SMILES string of drug compounds in combination with an array of various encoders, we were able to surpass the predictive performance reached by utilizing Morgan fingerprints (the baseline model). Notably, encoders based solely on attention mechanisms (i.e., SA and CA) exhibited superior performance compared to RNN or CNN encoders, indicating that drug sensitivity may be more predictable from molecular information on an atomic level rather than longer range dependencies. This observation however, must be further investigated and verified as a future direction. The atom-level attention weights obtained in our models may be used to identify atomic features or bonds that are deemed more informative by the algorithm. We illustrated the atom-level attention weights returned by our SA model for Tipifarnib and highlighted the atoms and bonds that were given a higher weight.

In addition, we devised and utilized a gene attention encoder that returned attention weights for genetic profile of cells and thereby enabled us to better interpret the results and identify genes that were most informative for IC50 prediction. As a testament to the validity of the gene attention weights, we observed that different cell lines of the same organ tend to have similar (but not the same) gene attention weights. We envision that the approach used in our attention-based gene encoder will be of great utility in deep learning applications where a high level of interpretability is desired. As a future direction, it would certainly be beneficial to include gene expression profiles from healthy cell lines in the training samples so as to ensure that the model extracts features that can differentiate between healthy and cancerous cells.

Due to the multi-modal nature of our models, the interpretability offered by the attention mechanism and the stringent evaluation criteria employed in training and evaluating our models, we envision our models to generalize well and be applicable in drug discovery or personalized medicine where estimates on efficacy of candidate compounds on a wide range of cancer cells are required.

References

- [1] Elina Petrova. Innovation in the pharmaceutical industry: The process of drug discovery and development. In *Innovation and marketing in the pharmaceutical industry*, pages 19–81. Springer, 2014.
- [2] Garrett B Goh, Nathan O Hodas, Charles Siegel, and Abhinav Vishnu. Smiles2vec: An interpretable general-purpose deep neural network for predicting chemical properties. *arXiv preprint arXiv:1712.02034*, 2017.
- [3] Ian Lloyd, Alexandra Shimmings, and Pink Sheet Scrip. Pharma r&d annual review 2017. Available at: pharmaintelligence.informa.com/resources/product-content/pharma-rd-annual-review-2018. Accessed [June 25, 2018], 2017.
- [4] Emily Hargrave-Thomas, Bo Yu, and Jóhannes Reynisson. Serendipity in anticancer drug discovery. *World journal of clinical oncology*, 3(1):1, 2012.
- [5] Mathew J Garnett, Elena J Edelman, Sonja J Heidorn, Chris D Greenman, Anahita Dastur, King Wai Lau, Patricia Greninger, I Richard Thompson, Xi Luo, Jorge Soares, et al. Systematic identification of genomic markers of drug sensitivity in cancer cells. *Nature*, 483(7391):570, 2012.
- [6] Wanjuan Yang, Jorge Soares, Patricia Greninger, Elena J Edelman, Howard Lightfoot, Simon Forbes, Nidhi Bindal, Dave Beare, James A Smith, I Richard Thompson, et al. Genomics of drug sensitivity in cancer (gdsc): a resource for therapeutic biomarker discovery in cancer cells. *Nucleic acids research*, 41(D1): D955–D961, 2012.
- [7] James C Costello, Laura M Heiser, Elisabeth Georgii, Mehmet Gönen, Michael P Menden, Nicholas J Wang, Mukesh Bansal, Petteri Hintsanen, Suleiman A Khan, John-Patrick Mpindi, et al. A community effort to assess and improve drug sensitivity prediction algorithms. *Nature biotechnology*, 32(12):1202, 2014.
- [8] Paul Geeleher, Nancy J Cox, and R Stephanie Huang. Cancer biomarker discovery is improved by accounting for variability in general levels of drug sensitivity in pre-clinical models. *Genome biology*, 17(1):190, 2016.
- [9] Michael P Menden, Francesco Iorio, Mathew Garnett, Ultan McDermott, Cyril H Benes, Pedro J Ballester, and Julio Saez-Rodriguez. Machine learning prediction of cancer cell sensitivity to drugs based on genomic and chemical properties. *PLoS one*, 8(4):e61318, 2013.
- [10] Mati Karelson, Victor S Lobanov, and Alan R Katritzky. Quantum-chemical descriptors in qsar/qspr studies. *Chemical reviews*, 96(3):1027–1044, 1996.
- [11] Adrià Cereto-Massagué, María José Ojeda, Cristina Valls, Miquel Mulero, Santiago Garcia-Vallvé, and Gerard Pujadas. Molecular fingerprint similarity search in virtual screening. *Methods*, 71:58–63, 2015.
- [12] Dzmitry Bahdanau, Kyunghyun Cho, and Yoshua Bengio. Neural machine translation by jointly learning to align and translate. *arXiv preprint arXiv:1409.0473*, 2014.
- [13] Hongming Chen, Ola Engkvist, Yinhai Wang, Marcus Olivecrona, and Thomas Blaschke. The rise of deep learning in drug discovery. *Drug discovery today*, 2018.

- [14] Philippe Schwaller, Theophile Gaudin, David Lanyi, Costas Bekas, and Teodoro Laino. “found in translation”: predicting outcomes of complex organic chemistry reactions using neural sequence-to-sequence models. *Chemical science*, 9(28):6091–6098, 2018.
- [15] David Rogers and Mathew Hahn. Extended-Connectivity Fingerprints. *Journal of Chemical Information and Modeling*, 50(5):742–754, May 2010. ISSN 1549-9596. doi: 10.1021/ci100050t. URL <https://doi.org/10.1021/ci100050t>.
- [16] M. P. Menden. *In silico models of drug response in cancer cell lines based on various molecular descriptors*. PhD thesis, University of Cambridge, 2016.
- [17] Ali Oskooei, Matteo Manica, Roland Mathis, and María Rodríguez Martínez. Network-based biased tree ensembles (NetBiTE) for drug sensitivity prediction and drug sensitivity biomarker identification in cancer. *arXiv preprint arXiv:1808.06603*, 2018.
- [18] Damian Szklarczyk, Andrea Franceschini, Stefan Wyder, Kristoffer Forslund, Davide Heller, Jaime Huerta-Cepas, Milan Simonovic, Alexander Roth, Alberto Santos, Kalliopi P Tsafo, et al. String v10: protein–protein interaction networks, integrated over the tree of life. *Nucleic acids research*, 43(D1): D447–D452, 2014.
- [19] Esben Jannik Bjerrum. Smiles enumeration as data augmentation for neural network modeling of molecules. *arXiv preprint arXiv:1703.07076*, 2017.
- [20] Matan Hofree, John P Shen, Hannah Carter, Andrew Gross, and Trey Ideker. Network-based stratification of tumor mutations. *Nature methods*, 10(11):1108, 2013.
- [21] Thomas Unterthiner, Andreas Mayr, Günter Klambauer, Marvin Steijaert, Jörg K Wegner, Hugo Ceulemans, and Sepp Hochreiter. Deep learning as an opportunity in virtual screening. In *Proceedings of the deep learning workshop at NIPS*, volume 27, pages 1–9, 2014.
- [22] Bharath Ramsundar, Steven Kearnes, Patrick Riley, Dale Webster, David Konerding, and Vijay Pande. Massively multitask networks for drug discovery. *arXiv preprint arXiv:1502.02072*, 2015.
- [23] Kyunghyun Cho, Bart Van Merriënboer, Caglar Gulcehre, Dzmitry Bahdanau, Fethi Bougares, Holger Schwenk, and Yoshua Bengio. Learning phrase representations using rnn encoder-decoder for statistical machine translation. *arXiv preprint arXiv:1406.1078*, 2014.
- [24] Robert Koprowski and Kenneth R Foster. Machine learning and medicine: book review and commentary, 2018.
- [25] Zichao Yang, Diyi Yang, Chris Dyer, Xiaodong He, Alex Smola, and Eduard Hovy. Hierarchical attention networks for document classification. In *Proceedings of the 2016 Conference of the North American Chapter of the Association for Computational Linguistics: Human Language Technologies*, pages 1480–1489, 2016.
- [26] Diederik P Kingma and Jimmy Ba. Adam: A method for stochastic optimization. *arXiv preprint arXiv:1412.6980*, 2014.
- [27] Ashish Vaswani, Noam Shazeer, Niki Parmar, Jakob Uszkoreit, Llion Jones, Aidan N Gomez, Łukasz Kaiser, and Illia Polosukhin. Attention is all you need. In *Advances in Neural Information Processing Systems*, pages 5998–6008, 2017.
- [28] Maxim V Kuleshov, Matthew R Jones, Andrew D Rouillard, Nicolas F Fernandez, Qiaonan Duan, Zichen Wang, Simon Koplev, Sherry L Jenkins, Kathleen M Jagodnik, Alexander Lachmann, et al. Enrichr: a comprehensive gene set enrichment analysis web server 2016 update. *Nucleic acids research*, 44(W1): W90–W97, 2016.
- [29] Michael Ashburner, Catherine A Ball, Judith A Blake, David Botstein, Heather Butler, J Michael Cherry, Allan P Davis, Kara Dolinski, Selina S Dwight, Janan T Eppig, et al. Gene ontology: tool for the unification of biology. *Nature genetics*, 25(1):25, 2000.
- [30] John J O’Shea, Daniella M Schwartz, Alejandro V Villarino, Massimo Gadina, Iain B McInnes, and Arian Laurence. The jak-stat pathway: impact on human disease and therapeutic intervention. *Annual review of medicine*, 66:311–328, 2015.
- [31] Ataman Sendoel, Joshua G Dunn, Edwin H Rodriguez, Shruti Naik, Nicholas C Gomez, Brian Hurwitz, John Levorse, Brian D Dill, Daniel Schramek, Henrik Molina, et al. Translation from unconventional 5 start sites drives tumour initiation. *Nature*, 541(7638):494, 2017.